Human Biodistribution and Dosimetry of the $D_{2/3}$ Agonist ^{11}C-*N*-Propylnorapomorphine (^{11}C-NPA) Determined from PET

Charles M. Laymon[1], N. Scott Mason[1], W. Gordon Frankle[1,2], Jonathan P. Carney[1], Brian J. Lopresti[1], Maralee Y. Litschge[1], Chester A. Mathis[1], James M. Mountz[1], and Rajesh Narendran[1]

[1]Department of Radiology, University of Pittsburgh, Pittsburgh, Pennsylvania; and [2]Department of Psychiatry, University of Pittsburgh, Pittsburgh, Pennsylvania

We measured the whole-body distribution of intravenously injected ^{11}C-*N*-propylnorapomorphine (^{11}C-NPA), a dopamine agonist PET tracer, in human subjects and determined the resulting absorbed radiation doses. **Methods:** Six subjects (3 women, 3 men) were injected with ^{11}C-NPA (nominal dose, 370 MBq). A total of 9 consecutive whole-body PET scans were obtained for each subject. In addition, time–activity curves for 12 organs were determined, and residence times were computed for each subject. Dosimetry was determined for the various body organs and the whole body. **Results:** The average NPA whole-body radiation dose was 3.17×10^{-3} mSv per MBq of injected ^{11}C-NPA. The organ receiving the highest dose was the gallbladder wall, with an average of 2.81×10^{-2} mSv·MBq^{-1}. **Conclusion:** On the basis of averaged dosimetry results, an administration of less than 1,780 MBq (<48 mCi) of ^{11}C-NPA yields an organ dose of under 50 mSv (5 rem) to all organs.

Key Words: molecular imaging; PET; radiobiology/dosimetry; dopamine; neuroreceptor

J Nucl Med 2009; 50:814–817
DOI: 10.2967/jnumed.108.058131

The G-protein–coupled receptor (GPCR) systems (e.g., the dopamine D_2 receptors) are configured in interconvertible states of high (D_{2high}) and low (D_{2low}) affinity for agonists (*1*) such as the PET radiotracer ^{11}C-*N*-propylnorapomorphine (^{11}C-NPA) (*2*). In contrast, antagonist radiotracers such as ^{123}I-iodobenzamide or ^{11}C-raclopride bind with equal affinity to D_{2high} and D_{2low} sites. The endogenous agonist dopamine is not expected to compete efficiently with antagonist radiotracers at the D_{2low} sites in studies measuring amphetamine (or stimulant)-induced dopamine transmission. However, agonist radiotracers that bind exclusively to D_{2high} sites are vulnerable to endogenous competition by dopamine. Thus, D_2 agonist radiotracers (e.g., NPA) may be superior for the measurement of amphetamine-induced dopamine release in humans. Early work (*2*) established the basic imaging-related properties of NPA, which suggest that this radiotracer may indeed be useful for assaying dopamine binding sites.

In conjunction with a human neuroresearch program, we have performed dynamic PET-based human biodistribution studies for intravenously injected NPA. The results were used to calculate radiation doses to various organs from the decay of the ^{11}C radiolabel (mode, 100% β^+ emission; half-life ($t_{1/2}$), 1,223 s; mean positron energy, 385.6 keV; endpoint energy, 960.2 keV) (*3*).

Received Sep. 15, 2008; revision accepted Jan. 28, 2009.
For correspondence or reprints contact: Charles M. Laymon, UPMC Presbyterian, Room B-938, 200 Lothrop St., Pittsburgh, PA 15213.
E-mail: CML14@pitt.edu

MATERIALS AND METHODS

Subjects

This work was performed under a University of Pittsburgh Institutional Review Board–approved protocol. Pregnant or breast-feeding subjects were excluded from this project. Subjects of childbearing potential underwent serum and urine pregnancy testing at the time they provided signed consent and on the day of the study. Three male and 3 female subjects completed the ^{11}C-NPA whole-body dosimetry PET studies. Table 1 lists subject demographics.

Radiochemistry

The preparation of ^{11}C-NPA is based on the work of Hwang et al. (*2*). Radiochemical yield averaged 9% at the end of synthesis based on ^{11}C. Specific activity at the end of synthesis was 81.4 ± 2.96 GBq/μmol (2.2 ± 0.8 Ci/μmol), and injected NPA mass was 2.4 ± 1.2 μg.

Scan Protocol

Each subject was scanned using an HR+ PET scanner (Siemens). Scans ranged from the top of the head to below the pelvis, using 7 bed positions. Before the radiotracer injection, 5 min per bed position of transmission data using the external ^{68}Ge sources of the scanner were acquired. Without altering the subject's position on the scanner bed, we administered an intravenous bolus injection of ^{11}C-NPA (nominal dose, 370 MBq). Scanning in 2-dimensional mode began 90 s later. The delayed scan start was incorporated into the protocol to allow close medical monitoring of the subject immediately after the tracer injection. For each subject, 9 whole-body scans were obtained. Data were acquired for 15 s/bed for scans 1 and 2, 30 s/bed for scans 3 and 4, 60 s/bed

TABLE 1. Research Subject Demographics

Subject no.	Sex	Height (cm)	Weight (kg)	Age (y)
1	F	161	69	22
2	F	168	66	38
3	F	170	73	39
4	M	180	82	20
5	M	175	64	24
6	M	180	80	21

for scans 5 and 6, 120 s/bed for scan 7, and 240 s/bed for scans 8 and 9.

Data Analysis

PET emission data were reconstructed with the manufacturer's software, using filtered backprojection with a 3-mm Hann filter. Each PET image was discretized into a 128 × 128 × 187 voxel volume with uniform voxel dimensions of 0.51 cm. Image processing included a measured attenuation correction using the acquired transmission data and corrections for scatter, random coincidences, and system deadtime. The process resulted in 9 whole-body image frames (1 for each scan) for each of the 6 subjects. As an aid to identifying organs, additional emission images were formed by summing time frames. Additionally, the transmission data from each subject were reconstructed to form a 511-keV attenuation image.

The transmission and summed images were used to identify 12 regions of tracer uptake (source organs) and generate regions of interest (ROIs) that were then applied to each time frame separately to obtain a time–activity curve for each of the 12 organs. Only those organs that either were identifiable from the transmission data or had tracer uptake significantly above background were used as source organs. The regions used were whole brain, cortical bone, liver, gallbladder, lower large intestine, upper large intestine, small intestine (represented by the duodenum), red marrow, heart, lungs, kidney, and bladder. The ROI generation and sampling used the technique described by Slifstein et al. (*4*). With the exception of the bladder, concentrations within each organ as a function of time were determined from a region placed well within the organ avoiding the organ boundaries. Total organ activities, except for cortical bone and red marrow volumes, were obtained using the standard male and female organ volumes given in Cristy and Eckerman (*5*); cortical bone and red marrow volumes were taken from Zankl et al. (*6*). The bladder, which is relatively hotter than and isolated from other sources of activity, was analyzed using an ROI slightly larger than the organ itself. In this case, the full measured bladder activity (concentration integrated over ROI volume) was used.

For these dosimetry studies, activity data uncorrected for radioactive decay were used. For each subject and each organ, a residence time, T_R, was calculated as:

$$T_R = \frac{\int_0^\infty A(t)dt}{NDf}, \qquad \text{Eq. 1}$$

where A(t) is the total activity in the organ as a function of time from the PET time–activity curves, D is the injected dose measured by the dose calibrator, N is the cross-calibration factor between the PET scanner and the dose calibrator used to assay subject dose, and f is a factor accounting for decay between the time of assay in the dose calibrator and the injection time. Integration was performed using the trapezoidal method and with the assumption of activity values of 0 at the 0 time point (the injection time). The contribution of the activity present after the last measured point was estimated analytically by assuming that the activity measured during the last of the 9 scans decayed with the $t_{1/2}$ of ^{11}C and that no transport of radioactivity occurred. In practice, this final contribution to residence time was not significant.

The cross-calibration factor, N, in Equation 1 was obtained in a phantom study using a 20-cm water-filled cylinder. A syringe containing 110 MBq of a ^{11}C solution was assayed in the facility dose calibrator. The ^{11}C was injected into the phantom, and the syringe was reassayed. A 2-bed-position emission scan, spanning the entire phantom volume, was obtained, followed by a transmission scan. These data were reconstructed in a manner similar to that of the human data. The total activity in the phantom as measured by the PET scanner was obtained using an ROI that was larger than the phantom. The dose calibrator/PET cross calibration factor was obtained by dividing the activity recovered in the PET image, corrected for decay, by the assayed activity from the dose calibrator.

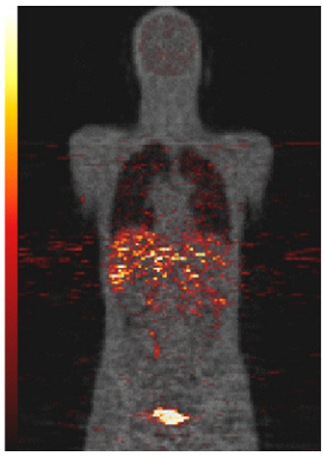

FIGURE 1. ^{11}C-NPA coronal PET image (hot metal scale) overlaid on attenuation image reconstructed from transmission data (gray scale) for male subject. PET data have been summed over first 4 scans and the image roughly represents activity distribution averaged over first 20 min after injection.

RGB

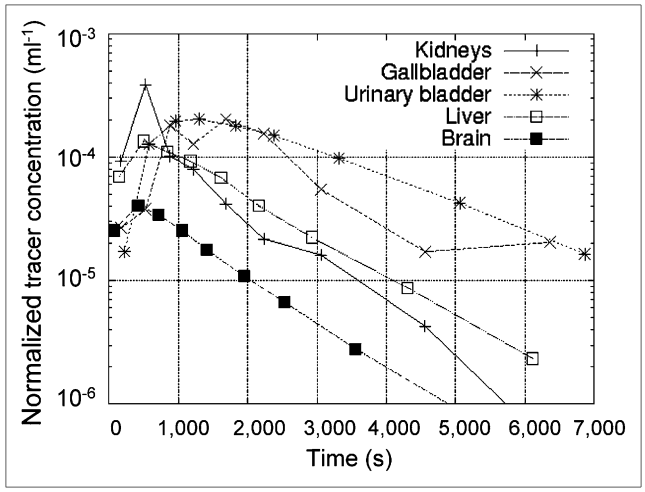

FIGURE 2. Activity concentration, normalized by injected dose, in various organs as function of time.

TABLE 2. Average Organ Residence Times

Organ	Residence time (s)
Liver	439.0
Duodenum	252.3
Urinary bladder	106.0
Kidney	97.6
Lung	89.9
Brain	77.2
Cortical bone	46.4
Gallbladder	33.3
Upper large intestine	30.4
Red marrow	25.0
Lower large intestine	17.9
Heart	13.5

In the case of loss of activity through decay only, the residence time for the whole body can be obtained from Equation 1 and is equal to the fixed value of $t_{1/2}/\ln 2$. Residence time unaccounted for in the 12 organs explicitly surveyed was assumed to be distributed throughout the rest of the body.

For each subject, dose calculations were made for organs throughout the body (target organs) using the program OLINDA (*7*), with the residence times from the source organs as input. The default male and female geometries were used in the calculation. OLINDA calculates radiation dose normalized to injected dose to each organ. It also reports a whole-body dose that is obtained by dividing the total absorbed energy (times a dimensionless radiation weighting factor, which for γ and β radiation is 1) by the modeled body mass. Thus, the whole-body radiation dose is a mass-weighted dose average. Additionally, OLINDA calculates an effective dose in which the organ doses (times the radiation weighting factor) are weighted by a risk factor (*8*) and summed together to produce a risk-weighted whole-body dose average.

RESULTS

Figure 1 is a coronal PET image from subject 6 (Table 1). The figure was produced by summing the first 4 PET scans and is an approximate representation of the activity concentration averaged over 1 $t_{1/2}$ of ^{11}C. The PET emission data are shown using a hot metal scale and superposed on an attenuation μ-value image for anatomic reference. Figure 2 is a semilog plot showing examples of time–activity curves from the same subject represented in Figure 1. Plots are shown for the 4 organs (urinary bladder, gallbladder, liver, and kidneys), with the highest peak-activity concentration of the 12 organs surveyed. Also shown are results for the brain. The time–activity curves for this subject are, for the most part, similar to those of the other subjects. Residence times are listed in Table 2 and have been averaged over all 6 subjects.

Table 3 lists organ radiation doses per injected dose as calculated by OLINDA given the residence times obtained from the measured NPA biodistributions. The results are broken down into β- and photon components. Values were

TABLE 3. Absorbed Radiation Dose Normalized to Injected Dose (mSv/MBq)

	Dose from...			
Target organ	β	Photon	Total	SD
Adrenals	5.12×10^{-4}	3.29×10^{-3}	3.80×10^{-3}	5.50×10^{-4}
Brain	3.65×10^{-3}	1.83×10^{-3}	5.48×10^{-3}	4.89×10^{-4}
Breasts	5.12×10^{-4}	9.68×10^{-4}	1.48×10^{-3}	2.57×10^{-4}
Gallbladder wall	1.99×10^{-2}	8.26×10^{-3}	2.81×10^{-2}	1.08×10^{-2}
LLI wall	4.46×10^{-3}	3.16×10^{-3}	7.62×10^{-3}	1.03×10^{-3}
Small intestine	1.99×10^{-2}	4.97×10^{-3}	2.48×10^{-2}	3.98×10^{-3}
Stomach wall	5.12×10^{-4}	2.17×10^{-3}	2.68×10^{-3}	3.78×10^{-4}
ULI wall	4.76×10^{-3}	5.45×10^{-3}	1.02×10^{-2}	2.14×10^{-3}
Heart wall	1.47×10^{-3}	2.20×10^{-3}	3.67×10^{-3}	4.35×10^{-4}
Kidneys	2.09×10^{-2}	6.34×10^{-3}	2.72×10^{-2}	5.72×10^{-3}
Liver	1.68×10^{-2}	8.27×10^{-3}	2.50×10^{-2}	4.44×10^{-3}
Lungs	6.24×10^{-3}	2.30×10^{-3}	8.54×10^{-3}	2.07×10^{-3}
Muscle	5.12×10^{-4}	1.43×10^{-3}	1.94×10^{-3}	2.70×10^{-4}
Ovaries	5.88×10^{-4}	3.84×10^{-3}	4.43×10^{-3}	2.10×10^{-4}
Pancreas	5.12×10^{-4}	3.09×10^{-3}	3.60×10^{-3}	4.87×10^{-4}
Red marrow	9.33×10^{-4}	1.84×10^{-3}	2.78×10^{-3}	6.87×10^{-4}
Osteogenic cells	2.39×10^{-3}	1.44×10^{-3}	3.83×10^{-3}	9.23×10^{-4}
Skin	5.12×10^{-4}	7.75×10^{-4}	1.29×10^{-3}	2.16×10^{-4}
Spleen	5.12×10^{-4}	1.93×10^{-3}	2.44×10^{-3}	3.77×10^{-4}
Testes	4.35×10^{-4}	9.07×10^{-4}	1.34×10^{-3}	1.45×10^{-4}
Thymus	5.12×10^{-4}	1.17×10^{-3}	1.68×10^{-3}	3.03×10^{-4}
Thyroid	5.12×10^{-4}	7.66×10^{-4}	1.28×10^{-3}	2.29×10^{-4}
Urinary bladder wall	1.82×10^{-2}	6.71×10^{-3}	2.49×10^{-2}	6.28×10^{-3}
Uterus	5.88×10^{-4}	3.85×10^{-3}	4.44×10^{-3}	2.06×10^{-4}
Total body	1.49×10^{-3}	1.68×10^{-3}	3.17×10^{-3}	4.01×10^{-4}

LLI wall = lower large intestine wall; ULI = upper large intestine wall.
The organ receiving the highest dose was the gallbladder wall. Final column lists standard deviation of total dose across subjects.

averaged over all subjects, except that doses to the testes were averaged over men only and doses to the ovaries and uterus were averaged over women only.

The average normalized whole-body dose in this study was 3.17×10^{-3} mSv·MBq^{-1} and spanned the range from 2.78×10^{-3} mSv·MBq^{-1} to 3.56×10^{-3} mSv·MBq^{-1}. The organ receiving the highest dose was the gallbladder wall, with an average value of 2.81×10^{-2} mSv·MBq^{-1}. The highest organ dose to an individual observed in this study was 4.52×10^{-2} mSv·MBq^{-1} to the gallbladder wall for a female subject. For the studies performed here, the average effective whole-body dose was 6.70×10^{-3} mSv·MBq^{-1}, with a low of 5.88×10^{-3} mSv·MBq^{-1} and a high of 8.00×10^{-3} mSv·MBq^{-1}.

DISCUSSION

A conservative approach was used in the dose calculations made in this work. The technique of sampling regions within organs reduces partial-volume or resolution effects (at least for organs sufficiently larger than the scanner resolution) that would otherwise tend to reduce the apparent activity concentrations within organs. Additionally, in implementing the method there was a tendency toward taking samples from hotter parts of the organ in cases of nonuniform distribution. Also, in performing calculations we ensured that no transport of radioactivity out of the body occurred by assuming that any radioactivity not explicitly accounted for in sampled organs was distributed uniformly throughout the unsampled organs, even though PET image analysis suggests that a small amount of activity is lost during the study, presumably via respiration.

Dosimetry calculations on several other ^{11}C-labeled neurotracers have been made (Supplemental Table 1; supplemental materials are available online only at http://jnm.snmjournals.org), with results that are similar to those reported here. To a large extent, dosimetry is determined simply by the $t_{1/2}$ of ^{11}C. For example, in the case of a hypothetical ^{11}C activity distribution taken to be uniform throughout the body, OLINDA calculates an effective dose of 3.30×10^{-3} mSv·MBq^{-1}, which is less than, but of a magnitude similar to, the values listed in Supplemental Table 1.

Our recent ^{11}C-NPA brain data (*9*) suggest that the minimum scanning duration necessary for reliable quantitation of ^{11}C-NPA binding is 60 min. Our proposed injection of 370 MBq (10 mCi) for a 60-min ^{11}C-NPA PET scan is consistent with the data published for other ^{11}C radiotracers such as ^{11}C-raclopride (*10*), (*S*)-(−)-*N*-([1-ethyl-2-pyrrolidinyl]-methyl)-5-bromo-[^{11}C]-2,3-dimethoxybenzamide (*11*), and *N*-{2-[4-(2-methoxyphenyl)piperaziny-1-yl]-ethyl}-*N*-(pyridin-2-yl)-cyclohexane-[^{11}C]carboxamide (*12*).

CONCLUSION

The human biodistribution of radioactivity as a function of time resulting from an intravenous injection of ^{11}C-NPA has been measured using PET, and dosimetry was determined. For the average over all 6 subjects, we found a whole-body exposure of 3.17×10^{-3} mSv per MBq of injected activity. The highest organ dose was to the gallbladder wall, which, on average, received 2.81×10^{-2} mSv per MBq of injected activity, and was considerably higher than doses to blood-forming organs, gonads, or the whole body. On the basis of these data and analysis, administration of less than 1,780 MBq (<48 mCi) of ^{11}C-NPA yields an organ dose of under 50 mSv (5 rem) (a commonly used organ dose limit [e.g., U.S. Title 21 CFR 361.1]) to all organs.

ACKNOWLEDGMENT

Financial support for this project was provided by National Institutes of Health grant MH068762.

REFERENCES

1. Zahniser NR, Molinoff PB. Effect of guanine nucleotides on striatal dopamine receptors. *Nature.* 1978;275:453–455.
2. Hwang DR, Narendran R, Huang YY, et al. Quantitative analysis of (-)-*N*-C-11-propyl-norapomorphine in vivo binding in nonhuman primates. *J Nucl Med.* 2004;45:338–346.
3. National Nuclear Data Center. Chart of Nuclides. Available at: http://www.nndc.bnl.gov/chart. Accessed February 25, 2009.
4. Slifstein M, Hwang DR, Martinez D, et al. Biodistribution and radiation dosimetry of the dopamine D_2 ligand ^{11}C-raclopride determined from human whole-body PET. *J Nucl Med.* 2006;47:313–319.
5. Cristy M, Eckerman KF. *Specific Absorbed Fractions of Energy at Various Ages from Internal Photon Sources. I. Methods.* Oak Ridge, TN: Oak Ridge National Laboratory; 1987.
6. Zankl M, Eckerman KF, Bolch WE. Voxel-based models representing the male and female ICRP reference adult: the skeleton. *Radiation Protect Dos.* 2007;127:174–186.
7. Stabin MG, Sparks RB, Crowe E. OLINDA/EXM: The second-generation personal computer software for internal dose assessment in nuclear medicine. *J Nucl Med.* 2005;46:1023–1027.
8. International Commission on Radiological Protection (ICRP). *1990 Recommendations of the International Commission on Radiological Protection.* ICRP Publication 60. New York, NY: Pergamon Press; 1991.
9. Narendran R, Frankle WG, Mason NS, et al. PET imaging of $D_{2/3}$ agonist binding in healthy human subjects with the radiotracer [^{11}C]-*N*-propyl-nor-apomorphine (NPA): preliminary evaluation and reproducibility studies. *Synapse.* March 19, 2009 [Epub ahead of print].
10. Drevets WC, Gautier C, Price JC, et al. Amphetamine-induced dopamine release in human ventral striatum correlates with euphoria. *Biol Psychiatry.* 2001;49:81–96.
11. Sudo Y, Suhara T, Inoue M, et al. Reproducibility of [C-11]FLB 457 binding in extrastriatal regions. *Nucl Med Commun.* 2001;22:1215–1221.
12. Parsey RV, Slifstein M, Hwang DR, et al. Validation and reproducibility of measurement of 5-HT1A receptor parameters with [carbonyl-C-11]WAY-100635 in humans: comparison of arterial and reference tissue input functions. *J Cereb Blood Flow Metab.* 2000;20:1111–1133.